

# Influence of covalence and anion symmetry on the structure of small metal hydroxide clusters: Sodium versus silver hydroxide

M. Bertolus<sup>a</sup>, V. Brenner, and P. Millié

Laboratoire de Chimie Théorique, DSM/DRECAM/SPAM, CEA-CE Saclay, 91191 Gif-sur-Yvette Cedex, France

Received 9 August 1999 and Received in final form 1st December 1999

**Abstract.** An *ab initio* study of the  $\text{Na}_n(\text{OH})_n$ ,  $\text{Na}_n(\text{OH})_{n-1}^+$ ,  $\text{Ag}_n(\text{OH})_n$ , and  $\text{Ag}_n(\text{OH})_{n-1}^+$  clusters with  $n$  up to four is presented. The results of this study show that, in accordance with experimental observations, the sodium hydroxide clusters are almost purely ionic, while the Ag–O bond exhibits a significant covalent character. The perturbation caused by the non-spherical  $\text{OH}^-$  group relatively to an atomic anion, as well as the influence on structures and energies of the covalent character of the metal-oxygen bond are determined. The appearance of metal-metal bonds in the silver hydroxide clusters is also discussed. Finally, the theoretical results obtained on the Na–OH clusters are compared to experimental results available on the dissociation of the  $\text{Na}_n(\text{OH})_{n-1}^+$  clusters.

**PACS.** 36.40.Mr Spectroscopy and geometrical structure of clusters – 36.40.Qv Stability and fragmentation of clusters

## Introduction

Recent experiments on sodium and silver hydroxide clusters [1,2] have revealed totally different behaviors for these two systems. First, experiments on metal-rich clusters [1] have shown that the  $\text{Na}_{p+q}(\text{OH})_q^+$  clusters exhibit the same stability pattern as a function of size as the pure metallic  $\text{Na}_p^+$  clusters. This can be explained by a segregation between a metallic part  $\text{Na}_p^+$  and a insulating part  $(\text{NaOH})_q$ , and suggests a strong ionic character of the Na–O bond. On the contrary,  $\text{Ag}_{p+q}(\text{OH})_q^+$  clusters exhibit “magic numbers” different from those observed for the pure  $\text{Ag}_p^+$  clusters, which suggests a more covalent character for the Ag–O bond. Second, experiments on the nucleation of silver clusters in the presence of oxygen and water [2] have shown that non-stoichiometric  $\text{Ag}_n\text{O}_x\text{H}_y$  clusters are formed, while only  $\text{Na}_n\text{O}_p^+$  and  $\text{Na}_n(\text{OH})_p^+$  are produced during the nucleation of sodium clusters.

A theoretical study will enable one to investigate the electronic, energetic and structural properties of these two systems to interpret these experimental results. From a theoretical standpoint, the study of Ag–OH and Na–OH clusters is also interesting since it enables one to gain further understanding of the ionic-covalent bond and, in particular, of the influence of the covalent part on the bond by studying two systems with different covalent characters. In addition, this study will allow us to determine the

perturbation of a non-spherical ionic group relative to an atomic anion on the structural and energetic properties.

We present here the first *ab initio* study of these systems concerning the small  $\text{Na}_n(\text{OH})_n$ ,  $\text{Na}_n(\text{OH})_{n-1}^+$ ,  $\text{Ag}_n(\text{OH})_n$ , and  $\text{Ag}_n(\text{OH})_{n-1}^+$  clusters with  $n$  up to four. First, the results on the Na–OH clusters are discussed. The comparison with the results obtained for “standard” ionic systems with an atomic anion yields the perturbation of the  $\text{OH}^-$  group. Second, we present the results on Ag–OH clusters and the conclusions we can draw on the influence of the covalent character of the metal-oxygen bond from the comparison of Na–OH and Ag–OH clusters.

## 1 Computational details

### 1.1 Strategy

To obtain the structures of the isomers for the  $\text{Na}_n(\text{OH})_n$ ,  $\text{Na}_n(\text{OH})_{n-1}^+$ ,  $\text{Ag}_n(\text{OH})_n$ , and  $\text{Ag}_n(\text{OH})_{n-1}^+$  with  $n \leq 4$ , we first implement a purely ionic potential for a M–X system, where  $\text{M}^+$  is a metal cation and  $\text{X}^-$  an atomic anion, in a program performing global explorations of potential energy surfaces [3]. In this potential the binding energy of a cluster relatively to the  $\text{M}^+$  and  $\text{X}^-$  ions is calculated as:

$$E = E_{\text{el}} + E_{\text{rep}} = \sum_{i < j} \frac{q_i q_j}{r_{ij}} + \sum_{\substack{j \in \text{M}^+ \\ j \in \text{X}^-}} A e^{-\frac{r_{ij}}{\beta}} \quad (\text{in au}). \quad (1)$$

In this equation, the charges  $q_i$  are fixed to +1 for  $\text{M}^+$  and to –1 for  $\text{X}^-$ , and  $A$  and  $\beta$  are parameters dependent from  $\text{M}^+$  and  $\text{X}^-$  obtained by fitting experimental

---

<sup>a</sup> Current address: CEA Cadarache, DCC/DESD/SEP/LEM, Bât. 108, 13108 Saint-Paul-Lèz-Durance, France.  
e-mail: bertolus@desdsud.cea.fr

data or results of *ab initio* calculations. The same structures are obtained using such a potential for various systems: Na–Cl [4,5], Na–F [6] or Li–H [7,8] and they are not modified when polarization energy is included [6]. Furthermore, these structures are very similar to those obtained using *ab initio* methods for very strongly ionic systems such as Na–Cl [9]. They are therefore considered as standard ionic structures and taken as starting structures for our study of the Na–OH and Ag–OH systems. In addition, starting structures for  $M_n(\text{OH})_{n-1}^+$  clusters are obtained by removing a OH group from some standard structures of  $M_n(\text{OH})_n$ . In each of these starting structures, the cations (M) are then replaced with Na or Ag atoms, and the anions (X) with oxygen. The metal-oxygen distances are then scaled to match the distances calculated in  $\text{Na}_2(\text{OH})_2$  and  $\text{Ag}_2(\text{OH})_2$ . These reference systems are chosen because the distances in the monomers are abnormally small. Hydrogen atoms are finally added to each oxygen atom at a distance of 0.97 Å, and as far as possible from its metal neighbors. All the obtained structures are then re-optimized at an *ab initio* level.

## 1.2 Ab initio method and basis sets

The second part of this work involves the study of the larger metal-rich clusters observed in the experiments of Bréchnignac *et al.* [2]. We have therefore chosen to use Density Functional Theory, and in particular the B3LYP functional [10,11] since it enables us to describe covalent, ionic, and metal-metal bonds at a reasonable computation cost and with similar accuracy [12–14].

Up to  $\text{Na}_3(\text{OH})_3$  and  $\text{Ag}_3(\text{OH})_3$ , geometries were optimized and energies calculated using B3LYP, while for the larger clusters energies were calculated using B3LYP at the geometries optimized in the Local Spin Density Approximation (VWN functional [15]). For Na–OH clusters, the nature of the obtained extrema was determined by calculating the vibration frequencies for the optimized geometry. Because of the cost of such calculations, no frequency was calculated for the Ag–OH clusters. The starting structures, however, were slightly distorted and optimized without symmetry restrictions. This should ensure that no saddle-point was obtained. All calculations were performed using the Gaussian 94 suite of programs [16].

Relatively small basis sets that could be used in the study of the larger clusters were chosen. For Na, all-electron calculations were performed using a standard 6-31G\* basis set to which a *d* polarization function (0.25) was added. This basis yields a  $\text{Na}^+$  polarizability equal to 0.86  $\text{au}^3$  and a Na ionization potential equal to 0.188 au, which compare well to the 1.01  $\text{au}^3$  [17] and 0.199 au [19] experimental values, respectively. Ag atoms were described using the relativistic pseudo-potential developed by LaJohn *et al.* for the 1*s*, 2*s*, 2*p*, 3*s*, 3*p*, and 3*d* electrons, and its associated basis (4*s*4*p*4*d*/3*s*2*p*3*d*) [19]. This pseudo-potential, which was developed for standard chemistry methods, also yields good results in DFT because it only freezes a relatively small number of electrons. The polarizability of  $\text{Ag}^{19+}$ , which is very small, is neglected.

**Table 1.** Comparison of bond lengths and angles obtained theoretically and experimentally for the NaOH and AgOH molecules.

	NaOH		AgOH	
	Th.	Exp. [20]	Th.	Exp. [21]
$r_{\text{M-O}}$ (Å)	1.926	1.95	2.071	2.016
$\theta_{\text{MOH}}$ (°)	180	180	111.4	108.3
$r_{\text{O-H}}$ (Å)	0.965	-	0.978	0.952

On the contrary, one should be cautious when using a pseudo-potential with only a valence electron, since the polarizability of  $\text{Ag}^+$ , which is relatively large (see below), is then neglected. This basis yields a Ag ionization potential equal to 0.277 au, which is in very good agreement with the 0.278 au experimental value [18]. The  $\text{Ag}^+$  polarizability calculated is 5.03  $\text{au}^3$ , which is only half the 10.03  $\text{au}^3$  experimental value [17], but is still much greater than the  $\text{Na}^+$  polarizability. The ratio calculated between  $\text{Ag}^+$  and  $\text{Na}^+$  polarizabilities is 6, compared to 10 seen experimentally. This polarizability value can only be improved by adding *f* orbitals to the basis set: adding three *f* orbitals (1.9653; 0.6517; 0.2210) to our basis set yields a  $\text{Ag}^+$  polarizability equal to 9.45  $\text{au}^3$ . This addition, however, increases the computation time dramatically, and would not allow us to study the silver hydroxide clusters up to  $\text{Ag}_4(\text{OH})_4$ . Finally, for O and H standard Pople 6-31G basis sets [20] completed by a polarization function (O: 0.165, H: 0.073) were used.

The geometries obtained using the method and basis sets chosen were compared to the only experimental data available on the structures, which concerns the NaOH [21] and AgOH molecules [22]. Table 1 shows a comparison of the bond lengths and angles obtained theoretically and experimentally for both molecules. It is seen that the calculation results, and especially the MOH angles, are in good agreement with the experimental data.

## 2 Results on Na–OH clusters

### 2.1 Population analysis and interpretation

Kohn-Sham orbitals being well-defined entities derived from the electronic density, they can be used in qualitative molecular orbital theory [23]. Population analyses such as Natural Bonding Orbital (NBO) analyses [24] can therefore be performed on these orbitals to confirm the strongly ionic behavior in the sodium hydroxide clusters. We carried out population analyses on various cluster sizes studied using the NBO method. The low population obtained for the 3*s* orbital of the Na atoms, between 0.02 and 0.08 in all the clusters studied, shows the strongly ionic character of the Na–O bond.

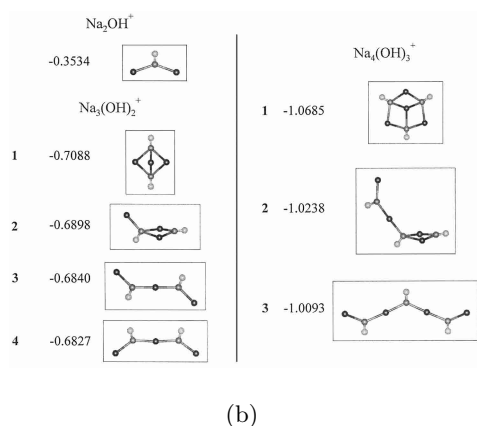
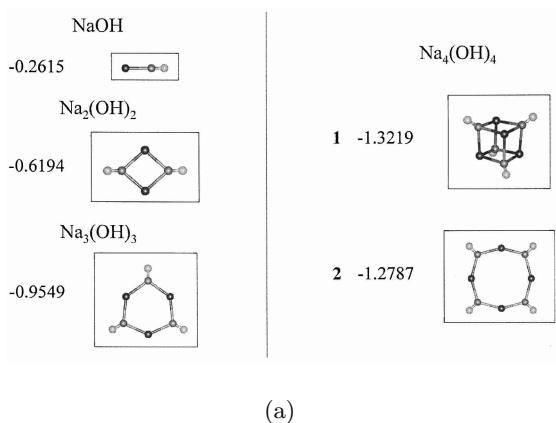


**Fig. 1.** (a) Structure and binding energy in atomic units of the isomers obtained for the  $\text{Na}_n(\text{OH})_n$  clusters with  $n \leq 4$ . (b) Structure and binding energy in atomic units of the isomers obtained for the  $\text{Na}_n(\text{OH})_{n-1}^+$  clusters with  $n \leq 4$ .

## 2.2 Isomers obtained and comparison with standard ionic clusters

We represented in Figures 1a and 1b the structures of the isomers obtained for the  $\text{Na}_n(\text{OH})_n$  and  $\text{Na}_n(\text{OH})_{n-1}^+$  clusters with  $n$  up to 4, as well as their binding energy relatively to  $\text{Na}^+$  and  $\text{OH}^-$ . Dark, medium, and light spheres represent sodium, oxygen, and hydrogen atoms, respectively. A comparison between the structures of the Na–OH clusters and the standard ionic ones [7,8] is also shown in Figure 2 for some representative isomers.

The structures obtained for Na–OH are very similar to the standard ionic structures, which is not really surprising, since the Na–O bond is strongly ionic. Steric effects due to the insertion of the H atoms, and electrostatic repulsion between Na and H, both positively charged, are responsible for the differences observed in the structures and in the energetic order. Standard ionic structures that do not have to be modified for the insertion of H atoms remain the same in the Na–OH system. This is the case for instance for the cyclic isomer of  $\text{Na}_2(\text{OH})_2$ , or for the most stable isomer of  $\text{Na}_4(\text{OH})_3^+$ . On the other hand, structures

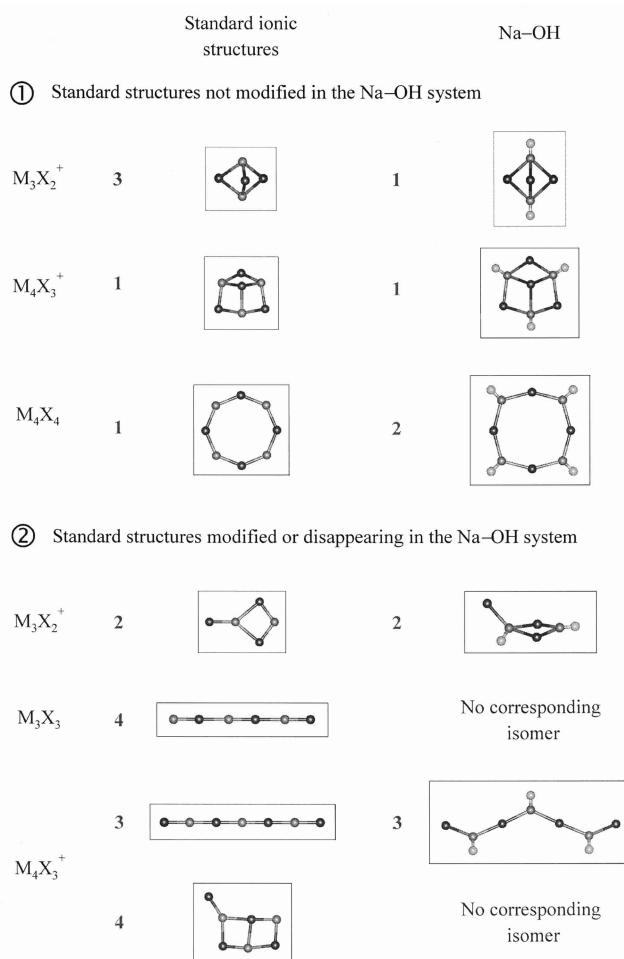


**Fig. 2.** Comparison of the structures obtained for the Na–OH clusters with the standard ionic structures.

in which there is not enough room to add H atoms, either disappear or are relatively strongly modified. Thus, the linear standard structures for  $\text{M}_2\text{X}^+$  and  $\text{M}_3\text{X}_2^+$  yield bent isomers for  $\text{Na}_2(\text{OH})^+$  and  $\text{Na}_3(\text{OH})_2^+$ . These isomers exhibit NaONa angles between 130 and 140°, which leaves room for the O–H bonds. Similarly, in the racket-shaped isomer of  $\text{Na}_3(\text{OH})_2^+$ , the terminal sodium atom is out of the plane defined by the 4-atom cycle because of the additional O–H bond. On the other hand, there are no pseudo-linear isomers for  $\text{Na}_2(\text{OH})_2$ ,  $\text{Na}_3(\text{OH})_3$ . Furthermore structures modified for the H insertion are all destabilized in the Na–OH system compared to the standard ionic ones, which yields different energetic orders for the two systems. For instance, in  $\text{Na}_3(\text{OH})_2^+$ , the trigonal bipyramidal isomer, the only structure not modified by the H addition, becomes the most stable. In  $\text{Na}_4(\text{OH})_3^+$ , the pseudo-planar isomer, which is unchanged by the H insertion, remains the most stable isomer. The number of structures concerned, however, is not enough so that we can conclude that this is a general rule.

The steric and electrostatic effects due to the H addition are likely to have significant consequences on the stability of larger compact isomers, which would contain

**Table 2.** Main products obtained experimentally in the dissociation of  $\text{Na}_n(\text{OH})_{n-1}^+$  clusters as a function of the size of the starting cluster.

Starting cluster	Products
$\text{Na}_{13}(\text{OH})_{12}^+$ , $\text{Na}_{17}(\text{OH})_{16}^+$	$\text{Na}_4(\text{OH})_4$ , $\text{Na}_2(\text{OH})_2$
$\text{Na}_7(\text{OH})_6^+$ , $\text{Na}_{16}(\text{OH})_{15}^+$	$\text{Na}_2(\text{OH})_2$
$\text{Na}_5(\text{OH})_4^+$	$\text{NaOH}$

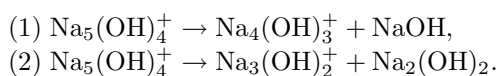
anions inside the structure, and not only on the surface as in the case of small clusters. In particular, the isomers formed by tridimensional cube stacking, which are widely observed in the standard ionic system, are likely to be destabilized. For instance, it will probably be difficult to form a cubic structure of  $\text{Na}_{14}(\text{OH})_{13}^+$  similar to the very stable structure observed in Li–H, Na–F or Na–Cl [6–9], since it ought to contain an  $\text{OH}^-$  group in the middle of the global cube. This is confirmed by the fact that Na–OH does not crystallize in a fcc lattice like Na–F or Li–H, but in a less compact orthorhombic one [25].

### 2.3 Comparison with experiment

The experiments carried out by Bréchnignac *et al.* on mass-selected clusters [1] yielded results on the dissociation of the  $\text{Na}_n(\text{OH})_{n-1}^+$  clusters with  $n$  up to twenty. In these experiments sodium hydroxide clusters are produced by mixing a few percents of water and oxygen with pure sodium clusters. They are then ionized and warmed up by a laser beam, mass-selected, and finally let to evaporate. The dissociation products are then analyzed in a time-of-flight spectrometer. Table 2 shows the main products obtained experimentally as a function of the starting cluster size. It can be seen that only  $\text{Na}_4(\text{OH})_4$  and  $\text{Na}_2(\text{OH})_2$  are obtained in the dissociation of large clusters whereas NaOH is the only product of the dissociation of  $\text{Na}_5(\text{OH})_4^+$ .

In order to compare our results with the experimental ones, as well as to better understand these differences between  $\text{Na}_5(\text{OH})_4^+$  and the larger clusters, we first calculated the energies of the dissociation paths for  $\text{Na}_5(\text{OH})_4^+$ . Second, if one considers the standard ionic structures for the larger clusters, and the fact that the larger Na–OH clusters dissociate in forming  $\text{Na}_4(\text{OH})_4$ , it can be assumed that they are at least partially cubic. Their dissociation can then be tentatively modeled by the dissociation of the cubic isomer of  $\text{Na}_4(\text{OH})_4$ , which we studied.

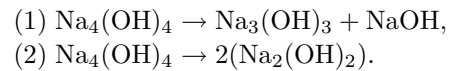
We first analyzed the dissociation of  $\text{Na}_5(\text{OH})_4^+$ . In this case, the sizes studied theoretically allow a direct comparison between the theoretical and experimental results. We considered the two dissociation paths, as follows,



Calculations of the energies of these two paths including zero-point energy (ZPE) corrections show that the first path is 0.003 au (0.09 eV) lower in energy than the second one. This result is in the same order of magnitude as

the accuracy that can be expected on the energy, but is still consistent with the fact that NaOH, not  $\text{Na}_2(\text{OH})_2$ , is observed. One can furthermore imagine that there is an energy barrier to the loss of  $\text{Na}_2(\text{OH})_2$ . The most stable isomer for  $\text{Na}_3(\text{OH})_2^+$  is the trigonal bipyramid, and we can make an assumption on the structure of the most stable isomer of  $\text{Na}_5(\text{OH})_4^+$ . According to our discussion in Section 2.2 there are only small differences between the standard and the Na–OH structures. Since the most stable structure for the standard  $\text{M}_5\text{X}_4^+$  is the pseudo-planar isomer, and since this structure is not modified by the insertion of hydrogen atoms, it is very probable that it is the most stable isomer for  $\text{Na}_5(\text{OH})_4^+$ . We see then that a significant reorganization would be necessary after the loss of  $\text{Na}_2(\text{OH})_2$ . On the contrary, almost no reorganization is needed to form the most stable of  $\text{Na}_4(\text{OH})_3^+$ , which is also pseudo-planar. This barrier would explain why only NaOH is observed during the dissociation of  $\text{Na}_5(\text{OH})_4^+$ .

Second, we studied the dissociation of  $\text{Na}_4(\text{OH})_4$ . We compared the two paths, as follows,



Calculations including ZPE corrections show that the first path is endothermic by 0.083 au (2.27 eV), while the second one is endothermic by 0.104 au (2.82 eV). The path leading to  $\text{Na}_2(\text{OH})_2$  is thus energetically more favorable by 0.020 au (0.55 eV). This is consistent with the fact that  $\text{Na}_2(\text{OH})_2$  is experimentally observed during the dissociation, and not  $\text{Na}_3(\text{OH})_3$  and NaOH. From a structural point of view, this energetically favorable path can be explained by the fact that the loss of  $\text{Na}_2(\text{OH})_2$  corresponds to the loss of a cube side, and that no reorganization is necessary for the remaining cubic part.

## 3 Results on Ag–OH clusters

### 3.1 Population analysis and interpretation

In order to compare the ionic character of the Ag–O and Na–O bonds, we also analyzed the electronic density in the Ag–OH clusters using the NBO method [24]. The population analysis for the AgOH molecule, in which the Ag–O distance calculated is short (2.07 Å), shows that the 5s orbital of the Ag atom contains 0.42 electrons, and that Ag is therefore relatively far from being an  $\text{Ag}^+$  ion. In fact, the situation is more complicated since a part of the 5s population comes from the depopulation of the 4d orbitals caused by the repulsion between the full 4d orbitals and the lone pairs of the O atom. This phenomenon, commonly observed in systems containing Ag [26] or Cu atoms [27], can be explained as follows. If the direction of the Ag–O bond is chosen as the  $z$ -axis, the orbital most strongly disturbed by the repulsion between the 4d orbitals and the O lone pairs is the  $d_{z^2}$  orbital, which points directly towards the O atom, and whose radial part is  $2z^2 - x^2 - y^2$ . The radial part of the 5s orbital is  $x^2 + y^2 + z^2$ . We see that combining linearly the 4d and 5s orbitals of the Ag atom,

$2z^2 - x^2 - y^2 - \lambda(x^2 + y^2 + z^2)$  makes it possible to decrease the  $z^2$  component, and therefore the repulsion between the  $d_{z^2}$  orbital and the lone pairs of the O atom. This enables the O and Ag atoms to come closer to each other, and stabilizes the Ag–O bond. This phenomenon occurs in all the clusters studied for all  $d$  orbitals pointing in the direction of the OH group. This means that the  $\text{Ag}^+ 4d^9 5s^1$  configuration, although relatively high in energy (approximately 0.2 au above the  $4d^{10} 5s^0$  ground configuration), plays a significant role in the Ag–O bond. It is, however, observed that the depopulation of the  $d$  orbital is in every case much smaller than the total  $5s$  population, so that Ag is always relatively far from an  $\text{Ag}^+$  ion. This means that the Ag–O bond is much less ionic than the Na–O bond. For instance, in the AgOH molecule, 0.07 electron is thus transferred from the  $d_{z^2}$  and  $d_{x^2-y^2}$  orbitals to the  $5s$  one, but 0.35 electrons actually coming from the  $5s$  orbital remain on the Ag atom. In  $\text{Ag}_2(\text{OH})_2$ , where the Ag–O distance is longer (2.22 Å), the population of the  $5s$  orbital is 0.23 electron, from which only 0.04 comes from the  $4d$  orbitals depopulation. In  $\text{Ag}_4(\text{OH})_3^+$ , the  $5s$  orbital contains 0.24 electron, from which 0.05 comes from the  $4d$  orbitals.

### 3.2 Isomers obtained and comparison with Na–OH

Figures 3a and 3b show the geometries and binding energies relatively to  $\text{Ag}^+$  and  $\text{OH}^-$  of the various isomers obtained for  $\text{Ag}_n(\text{OH})_n$  and  $\text{Ag}_n(\text{OH})_{n-1}^+$  with  $n$  up to four. Dark, medium, and light spheres represent silver, oxygen, and hydrogen atoms, respectively. In order to analyze the effects of the covalence in the Ag–O bond, we compared the Ag–OH and Na–OH clusters from energetic and structural standpoints.

The variation of the binding energy of the most stable isomer relatively to  $\text{Ag}^+$  and  $\text{OH}^-$  as a function of size is represented for the neutral clusters of the two systems in Figure 4. It is observed that for all sizes the binding energy of the Ag–OH clusters is larger than that of the Na–OH clusters, although the interatomic distances are slightly shorter in the latter. A quick calculation of the  $\text{Na}^+$  and  $\text{Ag}^+$  polarization energies per  $\text{OH}^-$  group using a  $-1$  charge on the oxygen atom shows that the difference in polarizability only accounts for 25% of the difference in the binding energy. This shows the significant stabilizing effect of the charge transfer in the Ag–O bond, and confirms the results of the population analysis. The relatively strong covalent character of the Ag–O bond also has an influence on the energetic order, which differs in the Na–OH and Ag–OH systems. For instance, there is an inversion between the planar and cubic isomers of  $\text{M}_4(\text{OH})_4$ , and a complete change of order between  $\text{Na}_3(\text{OH})_2^+$  and  $\text{Ag}_3(\text{OH})_2^+$  on the one hand, and between  $\text{Na}_4(\text{OH})_3^+$  and  $\text{Ag}_4(\text{OH})_3^+$  on the other hand. Finally, it can be noticed in Figure 4 that the energy variations for the two systems are practically parallel, except for  $\text{Ag}_3(\text{OH})_3$ , which seems to be particularly stable compared to  $\text{Na}_3(\text{OH})_3$ .

Looking at the geometries, one sees significant differences between the two systems. These differences can

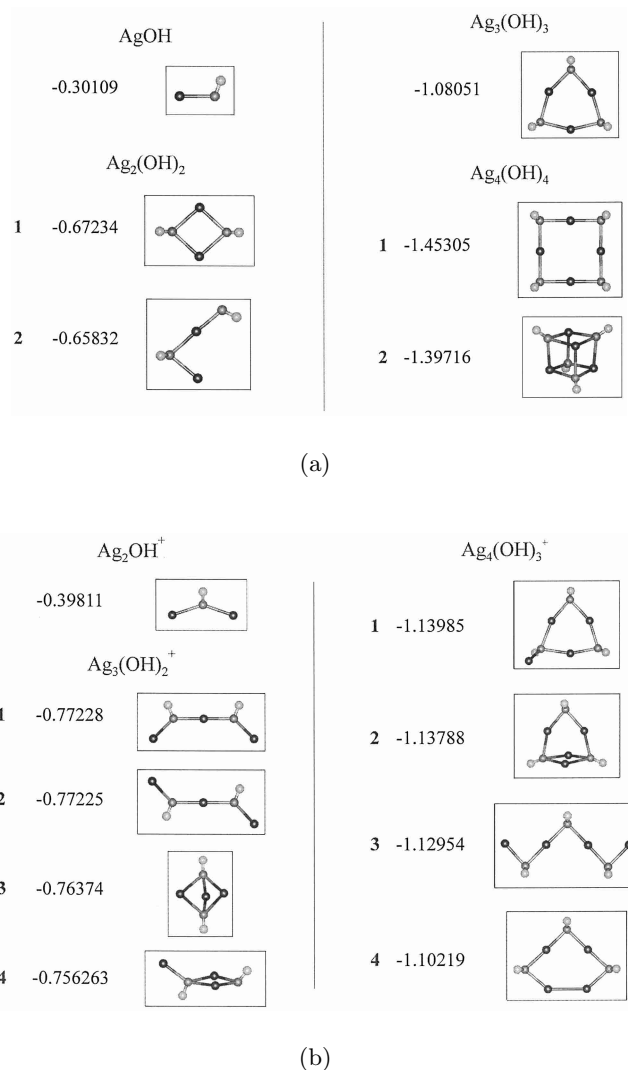


**Fig. 3.** (a) Structure and binding energy in atomic units of the isomers obtained for the  $\text{Ag}_n(\text{OH})_n$  clusters with  $n \leq 4$ . (b) Structure and binding energy in atomic units of the isomers obtained for the  $\text{Ag}_n(\text{OH})_{n-1}^+$  clusters with  $n \leq 4$ .

already be observed in the monomer, which is linear in NaOH, bent in AgOH. The structures of the Ag–OH clusters can still be derived from those of the Na–OH clusters, but three main differences are observed. Figure 5 shows some isomers of Na–OH and Ag–OH representative of the similarities and differences between the two systems. First, the H atoms are positioned differently relatively to the “skeleton” formed by the Ag and O atoms. In the Na–OH system the H atoms are positioned such as the dipole moment of the O–H bond is aligned with the total electric field. In Ag–OH it seems that their position is a compromise between the effect of the electric field and the influence of the charge transfer term. If we suppose that the oxygen is not hybridized, this term is maximal for an AgOH angle equal to  $90^\circ$  because the overlap between the  $5s$  Ag orbital and one of the oxygen  $2p$  lone

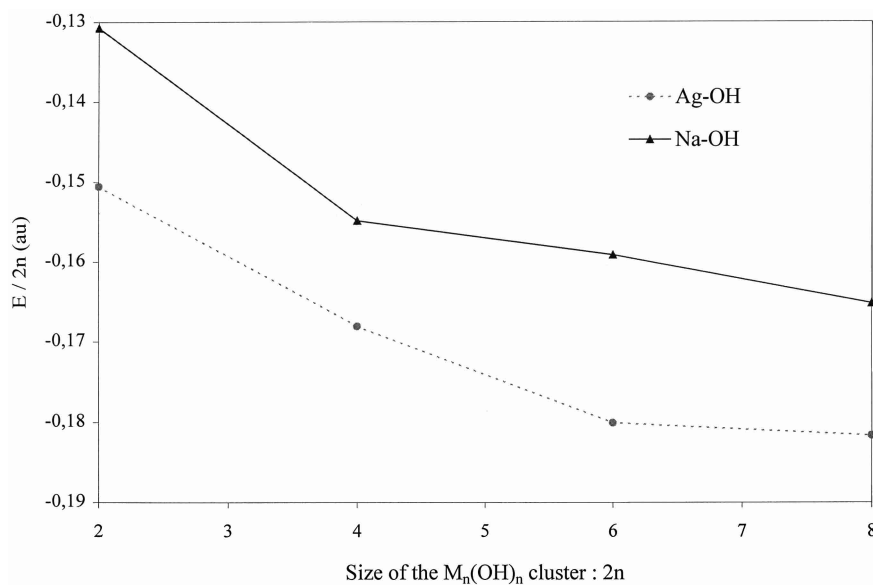


**Fig. 4.** Variation of the binding energy as a function of size in the neutral Na-OH and Ag-OH clusters.

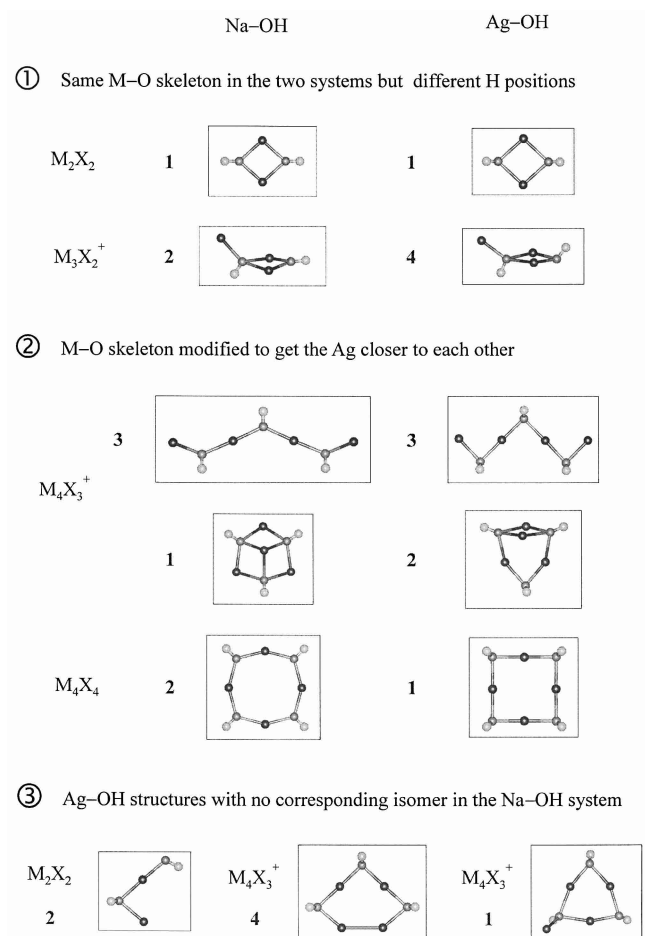


**Fig. 5.** Comparison of the structures obtained for the Na-OH and Ag-OH clusters.

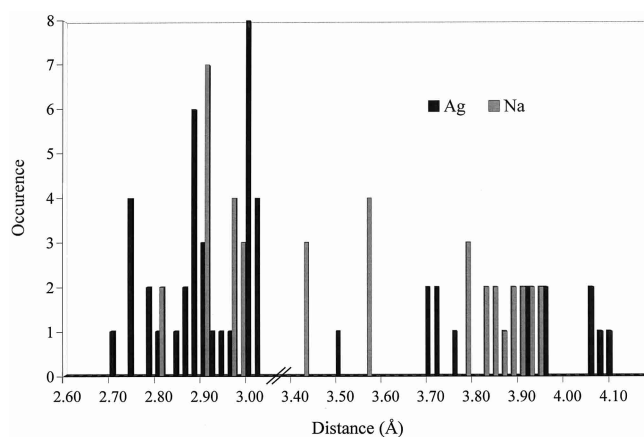


**Fig. 6.** Histogram of metal-metal distances in the Na-OH and Ag-OH clusters studied.

pairs is then maximal. This difference can for instance be seen in the racket-shaped isomer of  $M_3(OH)_2^+$ , where one of the H atoms is in the plane of the cycle in  $Na_3(OH)_2^+$ , while it is largely out-of-plane in  $Ag_3(OH)_2^+$ . Second, the AgOAg angles are much smaller than the NaONa ones: they are very often close to  $90^\circ$ , and smaller than  $130^\circ$  except in  $Ag_2OH^+$ . This is particularly visible in the case of the cyclic isomer of  $Ag_4(OH)_4$ , which is square-shaped, and not an almost regular octagon like the  $Na_4(OH)_4$  one. This enables the Ag atoms to get closer to each other, many Ag-Ag distances being relatively short compared to the  $2.63 \text{ \AA}$  equilibrium distance in  $Ag_2$ :  $2.71 \text{ \AA}$  in the second  $Ag_4(OH)_3^+$  isomer, and  $2.95 \text{ \AA}$  in the  $Ag_3(OH)_3$  cyclic isomer. Third, one can notice some Ag-OH isomers with no counterpart in the Na-OH system, which also exhibit short Ag-Ag distances: the first  $Ag_4(OH)_3^+$  isomer contains three Ag-Ag bonds close to  $2.75 \text{ \AA}$ , and the fourth

$\text{Ag}_4(\text{OH})_3^+$  isomer even exhibits two Ag atoms as first neighbors. The important difference between the two systems seems therefore to be the relatively short distances between atoms, and in particular between metal atoms, in the Ag–OH clusters. To quantify this phenomenon we took some statistics on the metal-oxygen metal-metal distances in the two systems. First, the average metal-oxygen bond length is very slightly smaller in Na–OH (2.14 Å) than in Ag–OH (2.15 Å), although the  $\text{Na}^+$  ionic radius (0.97 Å [18]) is significantly smaller than that of  $\text{Ag}^+$  (1.26 Å [18]). This confirms the partially covalent character of the Ag–O bond. Second, the average M–M bond length in all the obtained isomers is 3.57 and 4.16 Å in the Ag–OH and Na–OH clusters, respectively. Furthermore, it can be seen on the distribution of metal-metal bonds represented in Figure 6 that Ag–Ag bond lengths start at 2.71 Å *versus* 2.82 for Na–Na, and that 35 Ag–Ag distances are shorter than 3.05 Å, compared to only 16 Na–Na distances. This shows that the Ag atoms can get noticeably closer to each other than the Na atoms. The interaction between two Ag atoms has therefore a significant bonding character, unlike the interaction between Na atoms, which is repulsive. It has furthermore a stabilizing effect on certain structures, such as the pseudo-linear structures of the neutral clusters, which were not stable in the Na–OH system.

The energetic and above all structural differences between the Ag–OH and Na–OH systems are significant even for very small sizes, and increase with size, as it is particularly visible on the charged clusters. It can be assumed that the geometries of the Ag–OH clusters are going to move progressively away from the standard ionic geometries. There is in particular the possibility of forming attractive interactions between Ag atoms, which should increase the polymorphism in the Ag–OH system, and possibly yield to the formation of a metallic kernel in some structures. This difference in behavior between Na and Ag atoms is probably the cause of the different magic numbers observed in the metal-rich clusters of the two systems.

## Conclusion

The investigation of the Na–OH and Ag–OH clusters shows that the  $\text{Na}_n(\text{OH})_n$  and  $\text{Na}_n(\text{OH})_{n-1}^+$  clusters with  $n$  up to four are almost purely ionic, while the Ag–O bond exhibits a significant covalent character. First, in the case of the Na–OH systems, the perturbation caused by the  $\text{OH}^-$  group relatively to a atomic anion has been determined. It enables one to predict the structures of larger size clusters starting from standard ionic structures. Furthermore, the comparison between theoretical and experimental results shows that the *ab initio* results are in good agreement with the experimental observations, and enable us to interpret them. Second, in the case of the Ag–OH clusters, our study shows that if the ionic part of the Ag–O bond has the largest influence on the geometry for the very small sizes, the possibility of forming a covalent bond between Ag atoms increases the number of stable

structures. It therefore seems difficult to predict the structures for larger sizes.

The second part of this work is now the study of the larger and non-stoichiometric  $\text{Ag}_n\text{O}_x\text{H}_y$  clusters observed in the experiments carried out by Bréchnignac *et al.* [2] to gain further understanding of the phenomena involved during the nucleation of silver clusters in the presence of water and oxygen.

This research was supported by Oak Ridge National Laboratory, managed by Lockheed-Martin Energy Research Corporation for the Department of Energy under Contract No. DE-AC05-96OR22464.

## References

1. C. Bréchnignac, P. Cahuzac, I. Tignères, *Eur. Phys. J. D* **9**, 421 (1999).
2. C. Bréchnignac, P. Cahuzac, I. Tignères, *Chem. Phys. Lett.* **303**, 304 (1999).
3. M. Bertolus, V. Brenner, P. Millié, *Z. Phys. D* **39**, 239 (1997).
4. J. Diefenbach, T.P. Martin, *J. Chem. Phys.* **83**, 4585 (1983).
5. N.G. Phillips, C.W.S. Conover, C.A. Bloomfield, *J. Chem. Phys.* **94**, 4980 (1991).
6. F. Calvo, Ph.D. thesis, Université Paul Sabatier, Toulouse, 1998; private communication.
7. M. Bertolus, Ph.D. thesis, Université Paris-Sud Orsay, 1998.
8. M. Bertolus, V. Brenner, P. Millié (in preparation).
9. A. Ayuela, J.M. López, J.A. Alonso, V. Luaña, *Physica B* **212**, 329 (1995).
10. A.D. Becke, *J. Chem. Phys.* **98**, 5648 (1993).
11. C. Lee, W. Yang, R.G. Parr, *Phys. Rev. B* **37**, 785 (1988).
12. J. Harris, R.O. Jones, *J. Chem. Phys.* **70**, 830 (1979).
13. B. Delley, A.J. Freeman, D.E. Ellis, *Phys. Rev. Lett.* **50**, 488 (1983).
14. J. Bernholc, N.A.W. Holzwarth, *Phys. Rev. Lett.* **50**, 1451 (1983).
15. S.H. Vosko, L. Wilk, M. Nusair, *Can. J. Phys.* **58**, 1200 (1980).
16. M.J. Frisch, G.W. Trucks, H.B. Schlegel, P.M.W. Gill, B.G. Johnson, M.A. Robb, J.R. Cheeseman, T. Keith, G.A. Petersson, J.A. Montgomery, K. Raghavachari, M.A. Al-Laham, V.G. Zakrzewski, J.V. Ortiz, J.B. Foresman, J. Cioslowski, B.B. Stefanov, A. Nanayakkara, M. Challacombe, C.Y. Peng, P.Y. Ayala, W. Chen, M.W. Wong, J.L. Andres, E.S. Replogle, R. Gomperts, R.L. Martin, D.J. Fox, J.S. Binkley, D.J. Defrees, J. Baker, J.P. Stewart, M. Head-Gordon, C. Gonzalez, J.A. Pople, *Gaussian 94, révisions C.2 et E.2*, Gaussian, Inc., Pittsburgh, Pennsylvania (1995).
17. S. Fraga, J. Karwowski, K.M.S. Saxena, *Handbook of Atomic Data* (Elsevier Scientific Publishing Co., Amsterdam, 1976).
18. D.R. Lide, *CRC Handbook of Chemistry and Physics*, 78th edn. (CRC Press, Boca Raton, 1997).
19. L.A. LaJohn, P.A. Christiansen, R.B. Ross, T. Atashroo, W.C. Ermler, *J. Chem. Phys.* **87**, 2812 (1987).

20. W.J. Hehre, L. Radom, P.V.R. Schleyer, J.A. Pople, *Ab Initio Molecular Orbital Theory* (Wiley Interscience, New York, 1986).
21. P. Kuijpers, T. Topping, A. Dymanus, *Chem. Phys.* **46**, 4768 (1976).
22. C.J. Whitham, H. Ozeki, S. Saito, *J. Chem. Phys.* **110**, 11109 (1999).
23. E.J. Baerends, O.V. Gritsenko, *J. Phys. Chem. A* **101**, 5383 (1997).
24. E.D. Glendening, A.E. Reed, J.E. Carpenter, F. Weinhold, NBO version 3.1 (1992).
25. W.B. Pearson, C.B. Shoemaker, A.J. Frueh, *Structure Reports for 1967* (Oosthoek, Scheltema & Holkema, Utrecht, 1975), Vol. 32A.
26. E. Léon, V. Brenner, P. Millié, *J. Phys. Chem.* (to be published).
27. C.W. Bauschlicher Jr, S.R. Langhoff, H. Partridge, *J. Chem. Phys.* **94**, 2068 (1991).